

**A NEW MODEL FOR CO ORDERING AT HIGH COVERAGES ON
LOW INDEX METAL SURFACES: A CORRELATION BETWEEN
LEED, HREELS AND IRS**
I. CO adsorbed on fcc (100) surfaces *

J.P. BIBERIAN

*Faculté des Sciences de Luminy, Département de Physique, Case 901, F-13288 Marseille Cedex 9,
France*

and

M.A. VAN HOVE

*Materials and Molecular Research Division, Lawrence Berkeley Laboratory and Department of
Chemistry, University of California, Berkeley, California 94720, USA*

Received 20 October 1981

In this paper, we reexamine the surface structures of CO on (100) surfaces of copper, palladium, nickel and platinum. We use the types of site determined by High Resolution Energy Electron Loss Spectroscopy (HREELS), or Infra Red Spectroscopy (IRS), to propose new models for the arrangement of CO molecules at coverages exceeding 1/2, i.e. at coverages higher than those corresponding to simple structures $c(2 \times 2)$ and $p(2\sqrt{2} \times \sqrt{2})R45^\circ$. Laser simulations allow us to decide the validity of the proposed models. The consequences of these models are the existence of at most two adsorption sites at all coverages, and the existence of antiphase domains separated by walls to form the complex structures. The transition between two consecutive structures due to an increase of coverage is a unidirectional compression, generating more wall regions.

1. Introduction

The adsorption of CO on low index metal surfaces is a very unique system in surface crystallography because of the large number of substrates utilized and the great variety of surface sensitive techniques used for its analysis. In particular, Low Energy Diffraction (LEED) readily gives information on the unit cell, and by analysis of the $I-V$ curves, the position of the molecules within the unit cell can be determined, at least for the simple structures. On the

* Supported in part by the Director, Office of Energy Research, Office of Basic Energy Sciences and Materials Sciences Division of the US Department of Energy under Contract W-7405-ENG-48.

other hand, High Resolution Energy Electron Loss Spectroscopy (HREELS) or Infra Red Spectroscopy (IRS) have also been used to determine the adsorption sites of the CO molecules. These two types of technique are complementary, because LEED gives long range order information and HREELS or IRS short range order information. It is then of great interest to compare the results of both, and to try to build a structural model that explains the data of all these experiments for different substrates and different coverages. At present, there are inconsistencies in the structural models based on "pseudo-hexagonal" overlayers proposed in the literature.

Because of multiple diffraction effects, the analysis of the LEED patterns is not straightforward and the observed extra spots have been the object of a controversy, at least two solutions being possible:

- (i) The observed LEED patterns are composed of diffraction spots originating either from the substrate, or from the adsorbate or by double diffraction between the adsorbate and the substrate.
- (ii) There is a coincidence unit cell between the adsorbed layer and the substrate giving rise to a superstructure, all the extra spots being due to the existence of this coincidence unit cell.

These two interpretations, when brought to their logical conclusion, lead to the same result. However, the first one is normally used in a simplified form where only spots with appreciable intensity are taken into account; specifically, there are spots composed of linear combinations of substrate and adsorbate reciprocal lattice vector with small (h, k) indices.

There are two limits where the two models are easily seen to be identical: one is when the coincidence unit cell is small, for example a $c(2 \times 2)$ structure on a square lattice, or a $(\sqrt{3} \times \sqrt{3})R30^\circ$ structure on a hexagonal lattice, and the other is when the coincidence lattice is very large, and almost all the ad molecules are out of registry. The double diffraction model is commonly applied to a non-registered adsorbed phase, while the coincidence lattice model is most suitable to describe a registered or partially registered adsorbed phase depending on the length of the coincidence unit cell.

The interpretation of the LEED patterns for the adsorption of CO on low index metal surfaces has so far mainly used the double diffraction model. Out of the ten systems analyzed this way, there is a contradiction between LEED and HREELS or IRS for three systems, i.e. CO on Cu (100), Cu (111) and Ru (0001), where top site adsorption is determined by HREELS or IRS and two or more sites are deduced from the LEED patterns.

The purpose of this paper and the following papers [1] is to reexamine all the ten systems with the coincidence lattice model instead of the double diffraction model to show that there is no contradiction between LEED and HREELS or IRS for the three systems mentioned above, and that the seven other systems are almost identical in both models.

2. Analysis of the LEED patterns

As mentioned in the introduction, there are two possible ways of interpreting the LEED patterns, one is the double diffraction model and the other is the coincidence lattice model Fig. 1 describes for a one-dimensional system the consequences of the choice of the model. In fig. 1a, for a coverage of $\theta = 1/2$, all the admolecules are in site, and half of the substrate sites are occupied. At higher coverage, for instance $\theta = 2/3$, there are two possibilities as shown in figs. 1b and 1c. In fig. 1b, the distance b between the admolecules is kept constant and $b = \frac{3}{2}a$, where a is the distance between substrate sites, thus two different sites are populated. In fig. 1c, all the admolecules are adsorbed at equivalent sites (full circles), but the distances between the admolecules are a and $2a$. Because of possible repulsive interaction between nearest-neighbour admolecules, they might shift out of their position as indicated in fig. 1d. If the coverage increases and approaches 1, there is less and less difference between the two models as shown in figs. 1e and 1f for $\theta = 8/9$.

The “double diffraction” interpretation leads to a “compact model” for the adsorbed CO layer which forms a pseudohexagonal layer on the two-dimensional surface. The “coincidence lattice” interpretation leads to a “high symmetry model” for the adsorbed layer as introduced by Huber and Oudar [2], where the admolecules are in equivalent sites and the coincidence unit cell is of high symmetry.

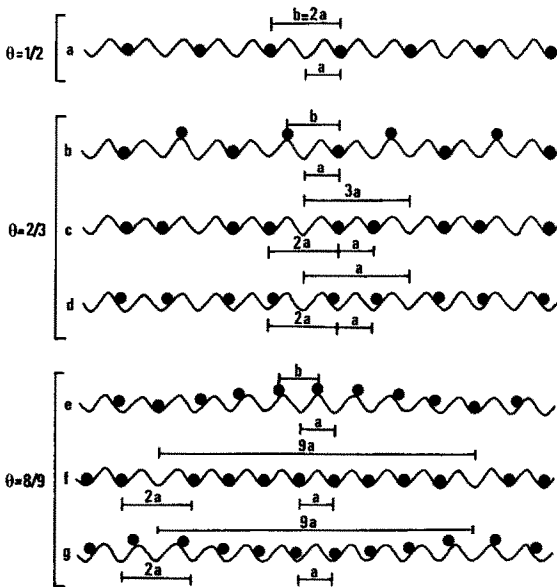


Fig. 1. One-dimensional model at three different coverages showing the differences between the compact model and the coincidence lattice model.

One motivation for the present work is the intriguing observation of a feature common to all LEED diffraction patterns that we have seen, published or otherwise available, for adsorbed CO molecules: the spot positions are such that all patterns can be explained by coincidence unit cells of finite size, i.e. of the commensurate superlattices form. The implication is that, as coverage increases, the coincidence unit cell changes in discrete steps from one commensurate size to the next, rather than in a continuous and smooth fashion. For example, CO on Pd (100) produces, with increasing coverage, successively $p(2\sqrt{2} \times 2\sqrt{2})R45^\circ$, $c(5\sqrt{2} \times \sqrt{2})R45^\circ$, $p(3\sqrt{2} \times \sqrt{2})R45^\circ$ and $c(7\sqrt{2} \times \sqrt{2})R45^\circ$ unit cells. Nevertheless, some authors have used the double diffraction interpretation, leading to a continuously and smoothly compressing pseudohexagonal CO lattice. In our view, the discreteness of the sequence of patterns is significant and leads to the more satisfactory results described in this paper.

One may wonder how the LEED patterns evolve from one finite unit cell to the next. It is known for simpler cases, such as a (2×1) to (3×1) transition, that the evolution from one unit cell to a closely related unit cell is relatively continuous, with spots moving gradually from one position to another position. However, during the transition, the spots are elongated in the direction of motion. This corresponds to a statistical mixture of the initial and final unit cells. We then conjecture that the reason for the discreteness in the available diffraction patterns for CO overlayers is due to attempts by the experimentalists to sharpen the spots: in those attempts the local coverage may unwillingly be adjusted to the nearest optimum value for a coincidence unit cell.

3. Principle of the analysis

In the case of CO adsorbed on metals, HREELS and IRS give a direct determination of the adsorption sites by the measurement of the C–O stretching frequency. Following a frequently used assignment, if the C–O stretching frequency is above 2000 cm^{-1} , the CO molecules are adsorbed on top sites, between 1700 and 2000 cm^{-1} they are adsorbed on bridge sites and below 1700 cm^{-1} on three-fold sites. These values are determined by IRS from metal carbonyl complexes and can vary from one metal to another.

For the LEED analysis, we use the coincidence unit cells determined by the diffraction pattern and build models with the CO molecules adsorbed in the sites determined by HREELS or IRS. We check the validity of such models by light scattering experiments (described in section 4).

It is well-known that multiple scattering effects are important in LEED, but they affect spot intensities much more than they affect the presence or absence of spots. So-called multiple scattering spots are usually already present kinematically as a result of substrate induced deformations of the adlayer. Therefore, the kinematical light diffraction is an adequate simulation of LEED

patterns. And since multiple scattering only modulates the kinematic intensities, there should be a direct correspondence between bright spots in the simulation and bright spots in the LEED pattern and also between faint spots in both situations (for this to be true, we must assume that the LEED patterns published and used to make structural statements are taken at representative energies where the relative spot intensities are typical of the entire energy range). Many successful laser diffraction simulations have already been performed which rely on the above assumption.

4. Laser simulation

In order to perform a kinematical analysis of the structure, the intensity of the diffraction spots can be calculated, or simulated, with a light scattering experiment. In our case, we have chosen this second solution, because it gives access to a pattern directly comparable with the LEED experiment. The diffraction grid is a photographic film with computer drawn transparent dots about 30 μm apart. Using a regular He-Ne laser giving a beam about 1 mm in diameter, we cover an area roughly 40 dots in diameter that corresponds in LEED to a crystal of about 100 \AA , i.e. of the order of the coherence length of the electron beam. So our laser simulation experiments are directly comparable to LEED.

To simulate the surface covered with CO, we have drawn the surface metal atoms with dots half the size of those used for the CO molecules. This choice is not important since the only aspect that has to be looked at is the relative intensity of the extra spots with respect to one another, and not with respect to the substrate spots. We shall see in the next sections that this qualitative comparison is sufficient to reduce the number of possible models to very few and sometimes only one. Some of our laser diffraction patterns show slight asymmetries even when the surface model is symmetrical, due to small inaccuracies in the small-scale computer plotting. Also the patterns are slightly distorted due to the positioning of the camera.

We should note that the accuracy of our comparison between LEED patterns and laser simulations is uncertain because the LEED patterns are taken from published photographs which give imprecise relative intensities of the LEED diffraction spots. It would be desirable to observe the diffraction patterns at all energies in order to determine if the spots are systematically intense or weak or even missing. Hopefully, this paper will incite authors with access to the original LEED photographs to check that our interpretation is consistent with those photographs.

5. Chemisorption of CO on (100) fcc metal surfaces

5.1. CO on Cu (100)

5.1.1. IRS and HREELS data

The adsorption of CO on Cu (100) has been studied by IRS [3–5] as well as by HREELS [6,7]. Both types of experiment show that there is only one peak for the C–O stretching frequency, namely at 2079 cm^{-1} as determined by IRS [5] or 2089 cm^{-1} as determined by HREELS [6,7], which position is independent of the coverage; by IRS, a 9 cm^{-1} shift is observed at high coverages. This behaviour is characteristic of a top site adsorption for the CO molecules at all coverages.

5.1.2. LEED observations and interpretations

LEED observations for CO adsorbed on Cu (100) have been made by various authors [3,7–12]. As the coverage increases, first a $c(2 \times 2)$ structure is observed that splits into a $c(7\sqrt{2} \times \sqrt{2})R45^\circ$ structure. Fig. 2 shows the schematic diagram of the LEED pattern corresponding to the $c(2 \times 2)$ and $c(7\sqrt{2} \times \sqrt{2})R45^\circ$ structures.

Possibly a $c(5\sqrt{2} \times \sqrt{2})R45^\circ$ is observed by Tracy [10] at higher coverages, as indicated in his work by arrows showing the displacement of the diffraction spots of the $c(7\sqrt{2} \times \sqrt{2})R45^\circ$ structure.

There is no ambiguity in interpreting the $c(2 \times 2)$ structure, with a coverage of $\theta = 0.5$: the CO molecules stand on top of the surface copper atoms. This is in agreement with the IRS [3–5] and HREELS [6] data and with the LEED intensity calculations [13].

The $c(7\sqrt{2} \times \sqrt{2})R45^\circ$ structure has been interpreted as a pseudohexagonal structure [10]. The reciprocal unit cell of the CO overlayer is drawn in fig. 2b. The two orthogonal domains are equivalent. Fig. 3a shows the position of the

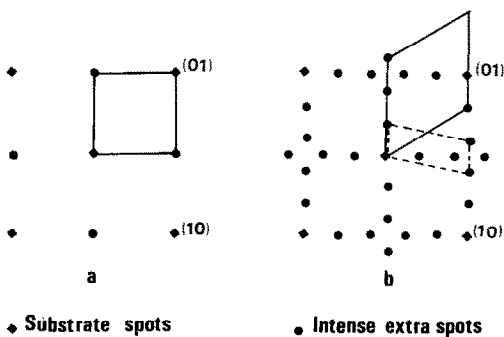


Fig. 2. Schematic representation of the LEED patterns observed when CO is adsorbed on Cu (100) surfaces: (a) $c(2 \times 2)$ pattern; (b) $c(7\sqrt{2} \times \sqrt{2})R45^\circ$ pattern. In full line, the pseudohexagonal unit cell; in dashed line, the coincidence lattice unit cell.

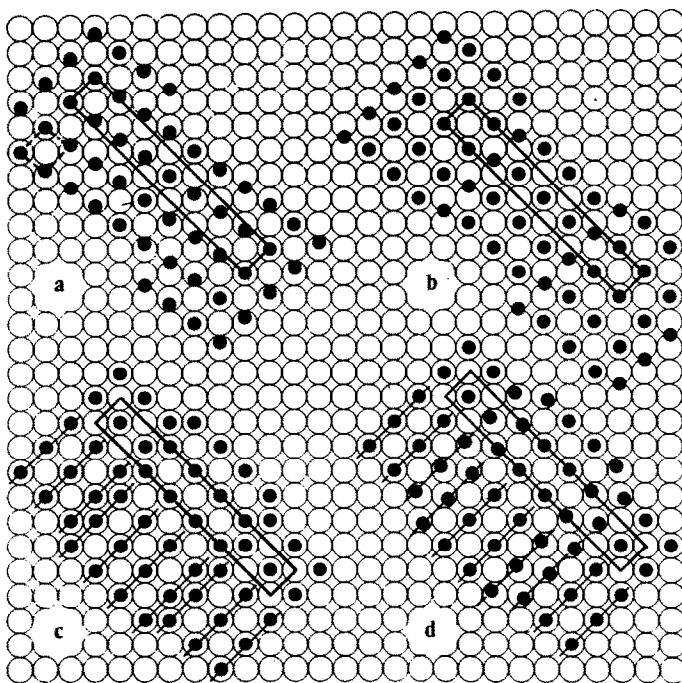


Fig. 3. Models proposed for the interpretation of the $c(7\sqrt{2} \times \sqrt{2})R45^\circ$ structure: (a) the CO molecules form a pseudo-hexagonal layer on top of the copper (100) surface; (b) a model with top and bridge sites; (c) a model with only top site adsorption formed by antiphase domains of $c(2 \times 2)$ strips having the $c2mm$ symmetry; (d) same as (c), but with a relaxation respecting the $c2mm$ symmetry.

CO molecules with respect to the copper substrate. In this interpretation, the weak extra spots are assumed to be multiple scattering spots.

In order to resolve a conflict between the LEED interpretation and work function measurements, Pritchard [12] has proposed another model with two types of site: top and bridge. Fig. 3b shows the position of the CO molecules with respect to the copper substrate. But there is no evidence by IRS or HREELS of the existence of bridged CO molecules. So, this model cannot be accepted.

The only model that can explain both the LEED observations and the IRS and HREELS spectra is shown in fig. 3c where all the CO molecules are on top sites and they form ordered antiphase domains of $c(2 \times 2)$ strips. A similar model has been proposed for the adsorption of sulfur on Fe (100) by Huber et al. [2] and lead on gold (100) by Biberian et al. [14]. This model has the highest symmetry compatible with the substrate, namely $C2mm$. The main argument against this model is that some of the CO molecules are separated by only 2.56

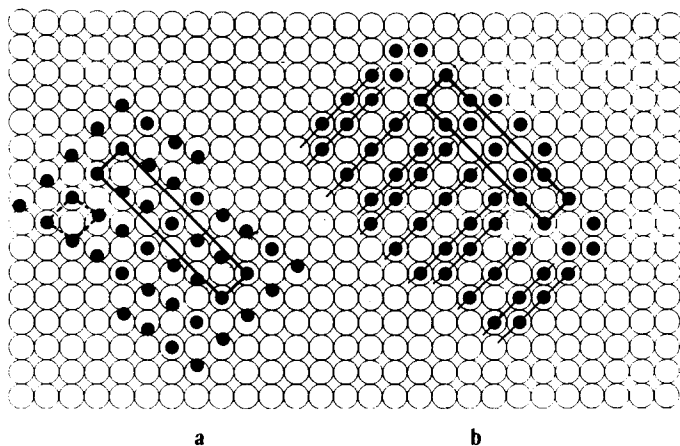


Fig. 4. Models proposed for the interpretation of the $c(5\sqrt{2} \times \sqrt{2})R45^\circ$ structure: (a) the CO molecules form a pseudo-hexagonal layer on top of the copper (100) surface; (b) a model with only top site adsorption formed by antiphase domains of $c(2 \times 2)$ strips having the $c2mm$ symmetry.

\AA , a distance much smaller than the Van der Waals radius of the CO molecules, 3.3 \AA . This point will be discussed in detail in section 7. However, a possible way of resolving this steric problem is a relaxation of the CO molecules either by a shift of some of the molecules keeping the C–O direction perpendicular to the surface, or by a tilt of the molecule, its direction being no more perpendicular to the surface, but still in a linearly bonded situation. One way of doing that is to relax the molecules into a pseudo-hexagonal arrangement similar to the one of fig. 3a. This operation has the disadvantage of breaking the $C2mm$ symmetry. Another relaxation of the CO molecules is described in fig. 3d that keeps the $C2mm$ symmetry, the molecules being translated along the mirror planes of the unit cell. This relaxation respects the top sites as necessitated by the HREELS and IRS data. It has to be pointed out that the four models of fig. 3 have the same coverage, $4/7$. The $c(5\sqrt{2} \times \sqrt{2})R45^\circ$ structure observed by Tracy [10] can be interpreted in a similar way to the $c(7\sqrt{2} \times \sqrt{2})R45^\circ$ structure. Fig. 4a shows the compact model associated with this structure and fig. 4b the 2D dislocation model. Here the $c(2 \times 2)$ strips are three atoms wide instead of four for the $c(7\sqrt{2} \times \sqrt{2})R45^\circ$ structure. Similar relaxations are possible. Here the coverage is $3/5$ for both models.

5.1.3. Laser simulations

Laser simulations of the models of fig. 3 for the $c(7\sqrt{2} \times \sqrt{2})R45^\circ$ structure are shown in fig. 5. It appears that the best fit with the LEED pattern (schematically drawn in fig. 2b) occurs for the model with top site adsorption

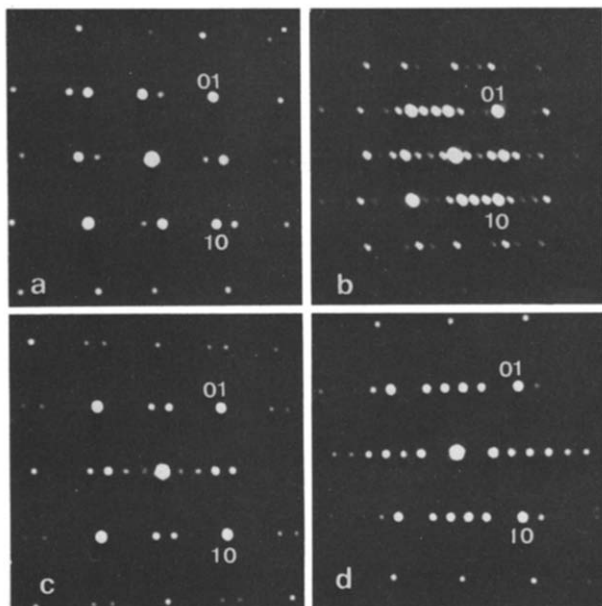


Fig. 5. Laser simulation of the models proposed in fig. 3. Only one overlayer orientation is shown, while LEED patterns normally show degenerate orientations related by 90° rotations and/or mirror plane operations.

without relaxation (fig. 3c). The laser diffraction pattern shows intense spots around the $(1/2, 1/2)$ positions as in the LEED pattern (there is only one domain in the laser simulation).

5.1.4. Conclusion

We have shown that for CO adsorbed on the (100) surface of copper, there is full agreement between LEED and HREELS or IRS with models based on adsorption of the CO molecules on top sites only. Better agreement between the LEED patterns and the laser simulation is obtained when there is no (or little) relaxation of the molecules to take into account the short distance (2.56 Å) between the molecules at the antiphase boundary. The sequence of LEED structures is described by creation of antiphase domains of $c(2 \times 2)$ as shown in fig. 3c. The domains are infinitely wide for the $c(2 \times 2)$ structure, 4 molecules wide for the $c(7\sqrt{2} \times \sqrt{2})R45^\circ$ structure and 3 molecules wide for the $c(5\sqrt{2} \times \sqrt{2})R45^\circ$ structure.

5.2. CO on Pd (100)

5.2.1. IRS data

The adsorption of CO on Pd (100) has been studied by IRS [15–17] at 300

K; the experiments show the presence of only one adsorption peak for the C–O stretching frequency whose position varies with increasing coverage from 1895 cm^{-1} at very low coverage ($\theta \approx 0.03$) to 1983 cm^{-1} at saturation ($\theta = 0.61$). This energy is characteristic of bridge site adsorption at all coverages. The shift with increasing coverage is due to lateral interactions, in part via the substrate.

5.2.2. LEED observations and interpretation

The adsorption of CO on Pd (100) has been studied by LEED [15–21]. With increasing coverage, the following sequence of patterns is observed: $p(2\sqrt{2} \times \sqrt{2})R45^\circ$, $c(5\sqrt{2} \times \sqrt{2})R45^\circ$, $p(3\sqrt{2} \times \sqrt{2})R45^\circ$ and $c(7\sqrt{2} \times \sqrt{2})R45^\circ$. Fig. 6 shows a schematic diagram of the LEED patterns corresponding to the various structures. The transitions between all these structures are continuous in the sense described in section 2.

At normal incidence, there are systematic extinctions in the $p(2\sqrt{2} \times \sqrt{2})R45^\circ$ structure indicating that the symmetry of the layer is $p2gg$ involving glide planes, and for the coverage $\theta = 0.5$ the only possible model is shown in fig. 7 where the CO molecules are in bridge sites, but in alternate directions [18]. This result is in agreement with the IRS spectra and LEED intensity calculations [22].

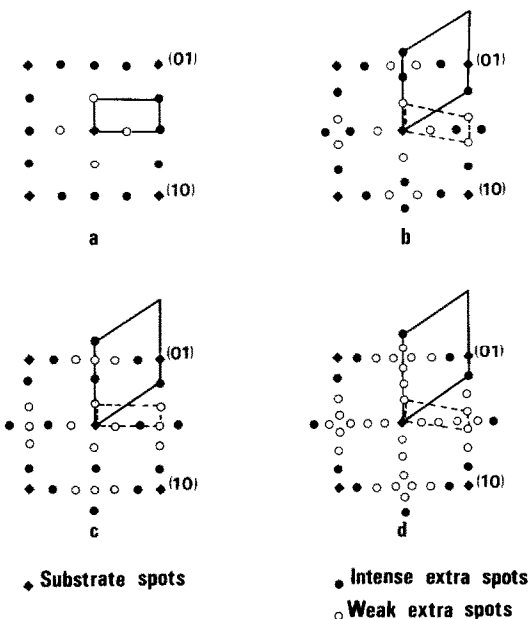


Fig. 6. LEED patterns for CO adsorbed on Pd (100): (a) $p(2\sqrt{2} \times \sqrt{2})R45^\circ$ structure, the extra spots represented by open circles are actually missing at normal incidence, indicating a $p2gg$ symmetry for the adlayer; (b) $c(5\sqrt{2} \times \sqrt{2})R45^\circ$ structure; (c) $p(3\sqrt{2} \times \sqrt{2})R45^\circ$ structure, same comments as for (a); (d) $c(7\sqrt{2} \times \sqrt{2})R45^\circ$ structure.

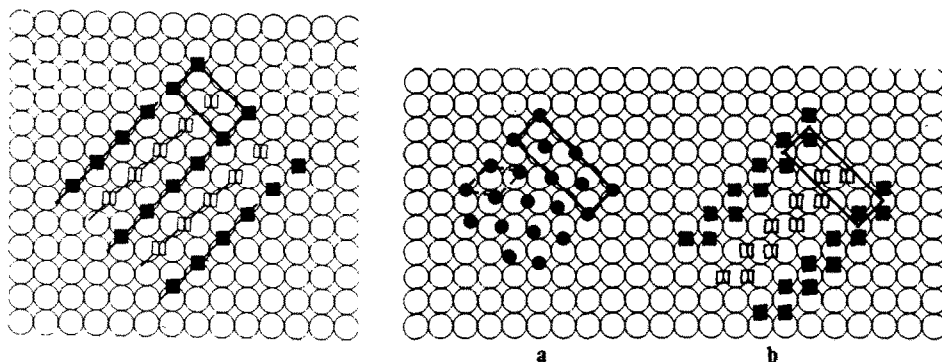


Fig. 7. CO/Pd (100) – the $p(2\sqrt{2} \times \sqrt{2})R45^\circ$ structure – model with all the molecules adsorbed on bridge sites, with the $p2gg$ symmetry. The CO molecules represented by full squares are not identical to those represented by open squares.

Fig. 8. CO/Pd (100) – the $c(5\sqrt{2} \times \sqrt{2})R45^\circ$ structure – (a) a compact model; (b) coincidence lattice model with all molecules in bridge sites.

The next structure, $c(5\sqrt{2} \times \sqrt{2})R45^\circ$, can be interpreted with a compact model [19]; the reciprocal unit cell is represented in fig. 6b and the direct lattice in fig. 8a. A small relaxation of this structure gives the model with all CO molecules on bridge sites as shown in fig. 8b. This structure has the high $c2mm$ symmetry.

The next structure, $p(3\sqrt{2} \times \sqrt{2})R45^\circ$, can be interpreted in the same way with a compact model [19] whose reciprocal unit cell is shown in fig. 6c and the direct lattice in fig. 9a using a compact model. A small relaxation of the CO molecules gives the model shown in fig. 9b with all CO molecules sitting on

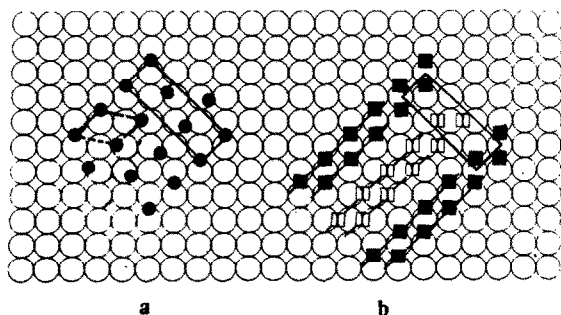


Fig. 9. CO/Pd (100) – the $p(3\sqrt{2} \times \sqrt{2})R45^\circ$ structure – (a) a compact model; (b) coincidence lattice model with all molecules in bridge sites.

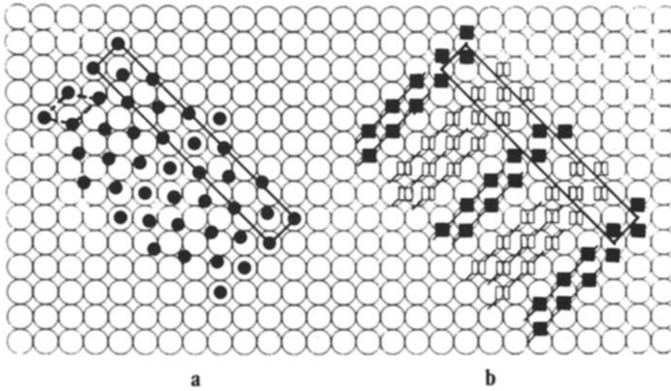


Fig. 10. CO/Pd (100) – the $c(7\sqrt{2} \times \sqrt{2})R45^\circ$ structure – (a) a compact model; (b) coincidence lattice model with all molecules in bridge sites.

bridge sites. This structure has the $p2gg$ symmetry.

The saturation structure $c(7\sqrt{2} \times \sqrt{2})R45^\circ$ can be interpreted in a way similar to the $c(5\sqrt{2} \times \sqrt{2})R45^\circ$ and $p(3\sqrt{2} \times \sqrt{2})R45^\circ$ structures. Fig. 6d shows the reciprocal lattice, while the compact model and the coincidence lattice unit cell model are shown in fig. 10.

5.2.3. Laser simulations

Fig. 11 shows the laser simulation patterns corresponding to the non-relaxed models with all the CO molecules on bridge sites. For the three structures $c(5\sqrt{2} \times \sqrt{2})R45^\circ$, $p(3\sqrt{2} \times \sqrt{2})R45^\circ$ and $c(7\sqrt{2} \times \sqrt{2})R45^\circ$, there is agreement between the relative intensities of the LEED patterns sketched in fig. 6 and the laser simulations of fig. 11 (only one domain orientation is present in the laser simulations).

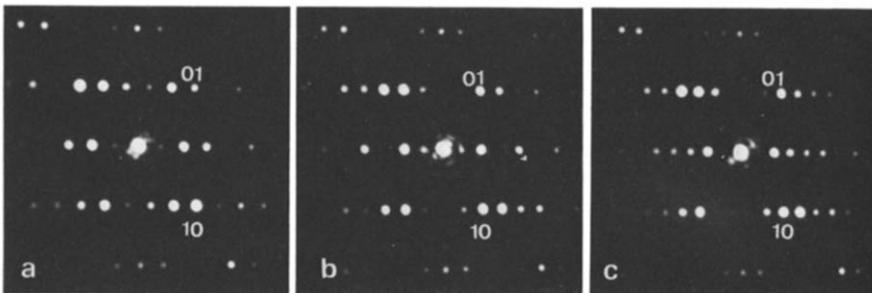


Fig. 11. Laser simulations of the coincidence lattice models with bridge site adsorption: (a) the $c(5\sqrt{2} \times \sqrt{2})R45^\circ$ structure; (b) the $p(3\sqrt{2} \times \sqrt{2})R45^\circ$ structure; (c) the $c(7\sqrt{2} \times \sqrt{2})R45^\circ$ structure.

5.2.4. Conclusion

For CO adsorbed on palladium (100) surfaces, there is full agreement between the LEED and IRS data, using models involving only bridge sites adsorption. The $p(2\sqrt{2} \times \sqrt{2})R45^\circ$ structure at half coverage is formed by alternate rows of CO molecules sitting on the two types of bridge site; for this structure, the ratio between the two types of sites is 1:1. The next structure, $c(5\sqrt{2} \times \sqrt{2})R45^\circ$, is formed by antiphase domains of $p(2\sqrt{2} \times \sqrt{2})R45^\circ$ strips; the ratio between the two types of bridge site is 1:2. The $p(3\sqrt{2} \times \sqrt{2})R45^\circ$ is also composed of antiphase domains of $p(2\sqrt{2} \times \sqrt{2})R45^\circ$ strips, but the ratio is now 2:2. The saturation structure $c(7\sqrt{2} \times \sqrt{2})R45^\circ$ is similar to the other ones, but the ratio is 2:3. Another way of looking at this series of structures is to observe that the boundaries between the $p(2\sqrt{2} \times \sqrt{2})R45^\circ$ strips are areas where the CO molecules form (1×1) structures and as a consequence the intermediate structures are in fact mixtures of $p(2\sqrt{2} \times \sqrt{2})R45^\circ$ and (1×1) structures.

5.3. CO on Ni (100)

5.3.1. IRS and HREELS data

The adsorption of CO on Ni (100) has been studied by HREELS [23,24] at 173 and 293 K, and by IRS [25] at 200, 230 and 285 K. Up to a coverage of $\theta = 0.5$, there is only one peak at 2068 cm^{-1} for the CO stretching frequency, indicating top site molecules. But at saturation, both top and bridge sites are present, the frequency associated with the bridge sites being at 1931 cm^{-1} . There is almost no shift of either peak with coverages.

5.3.2. LEED observations and interpretation

The adsorption of CO on Ni (100) has been studied by LEED [13,26–33].

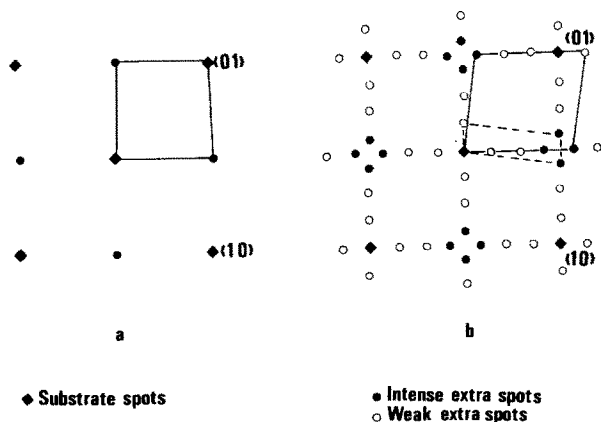


Fig. 12. LEED patterns for CO adsorbed on Ni (100): (a) $c(2 \times 2)$ structure; (b) $c(5\sqrt{2} \times \sqrt{2})R45^\circ$ structure.

At $\theta = 0.5$, a $c(2 \times 2)$ structure is observed and at $\theta = 0.6$, a $c(5\sqrt{2} \times \sqrt{2})R45^\circ$ structure. Tracy [29] also reports the existence of a compressed structure at $\theta = 0.68$ whose notation would be $p(3\sqrt{2} \times \sqrt{2})R45^\circ$. Fig. 12 shows the LEED diagrams associated with the first two structures.

There is no ambiguity in determining the arrangement of the CO molecules corresponding to the $c(2 \times 2)$ structure. As determined by HREELS [23,24] or IRS [25] and LEED intensity calculations [30–33], the CO molecules are on top sites.

Fig. 13a shows a possible model for interpreting the $c(5\sqrt{2} \times \sqrt{2})R45^\circ$ structure with a slightly relaxed compact model. Figs. 13b and 13c show two possible ways of having top and bridge sites, with 2 bridge sites for each top site, while fig. 13d shows a possible arrangement with 2 top sites for each bridge site.

5.3.3. Laser simulation

Fig. 14 shows the laser diffraction patterns corresponding to the models described in fig. 13. The only model that does not give a laser diffraction

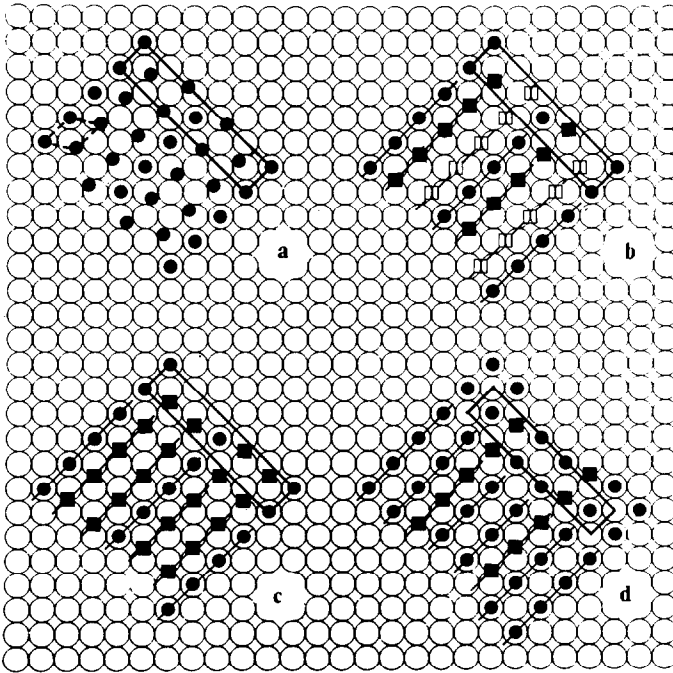


Fig. 13. CO/Ni(100) – $c(5\sqrt{2} \times \sqrt{2})R45^\circ$ structure – (a) a compact model, (b) and (c) coincidence lattice models with top and bridge sites, with one top site for two bridge sites; (d) coincidence lattice models with top and bridge sites, with two top sites for one bridge site.

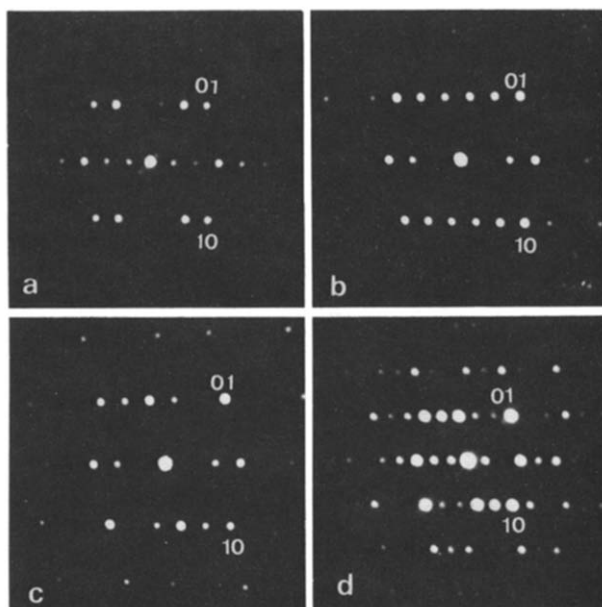


Fig. 14. Laser simulations of the models of the $c(5\sqrt{2} \times \sqrt{2})R45^\circ$ structure represented in fig. 13.

pattern similar to the LEED pattern is the hexagonal model (fig. 13a). The three other models give laser simulation patterns compatible with the LEED.

5.3.4. Conclusion

At half coverage, CO forms on nickel (100) surfaces a $c(2 \times 2)$ structure, with all the CO molecules on top sites. At higher coverage, a $c(5\sqrt{2} \times \sqrt{2})R45^\circ$ structure appears with top and bridge sites. From our laser simulations, it is not possible to determine which of the three models proposed in figs. 13b–13d is better. But the hexagonal model (fig. 13a) is not adequate. The three models of figs. 13b–13d have bridge and top sites only.

5.4. CO on Pt (100)

5.4.1. HREELS data

The adsorption of CO on Pt (100) has been studied by HREELS [34,35] on the reconstructed as well as on the unreconstructed surfaces at 300 and 150 K. For the reconstructed surface, at low coverage, there is only one peak for the CO stretching frequency at 2089 cm^{-1} , corresponding to top sites, and at high coverage, a second peak appears at 1971 cm^{-1} , corresponding to bridge sites. For the unreconstructed surface, bridge sites are present at low coverage as well as top sites. At higher coverages, spectra of the reconstructed and

non-reconstructed surfaces are identical as expected since the reconstruction is removed by the adsorption of CO.

5.4.2. LEED observations and interpretation

The adsorption of CO on Pt (100) has been studied by LEED on the reconstructed [36,37] and the unreconstructed [38,39] surfaces. At coverage $\theta = 0.5$, a $c(2 \times 2)$ structure is observed only on the unreconstructed surface. For $\theta = 2/3$, a $p(3\sqrt{2} \times \sqrt{2})R45^\circ$ structure is observed for both surfaces (the reconstruction having disappeared) and at $\theta = 3/4$ a $c(4 \times 2)$ structure appears again for both surfaces. Fig. 15 shows the sequence of the LEED patterns observed.

Since the $c(2 \times 2)$ structure appears only on the unreconstructed surface, where mainly bridge site CO are present according to the HREELS data [34,35], there is no ambiguity in determining the structure associated with the

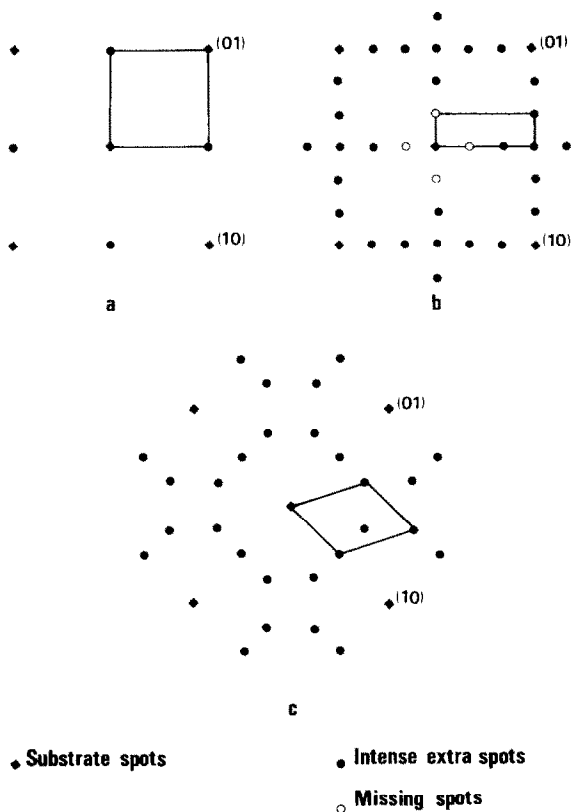


Fig. 15. LEED patterns for CO adsorbed on Pt (100): (a) $c(2 \times 2)$ structure; (b) $p(3\sqrt{2} \times \sqrt{2})R45^\circ$ structure, the open circles are missing extra spots; (c) $c(4 \times 2)$ structure.

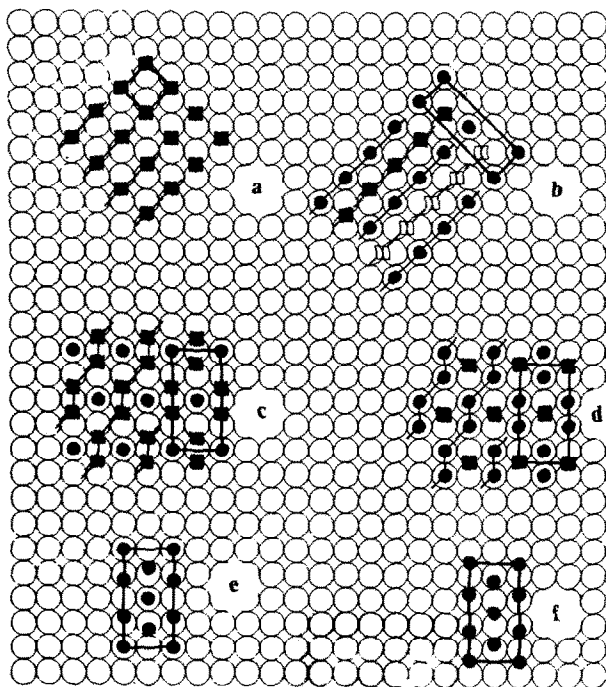


Fig. 16. CO/Pt (100): (a) $c(2 \times 2)$ structure with bridge site adsorption; (b) $p(3\sqrt{2} \times \sqrt{2})R45^\circ$ with top and bridge site adsorption; (c) and (d) $c(4 \times 2)$ structure with top and bridge sites; (e) and (f) same as (c) and (d) after relaxations leading to compact models.

$c(2 \times 2)$ structure as shown in fig. 16a. There is only one model to interpret the $p(3\sqrt{2} \times \sqrt{2})R45^\circ$ structure with bridge and top sites, as shown in fig. 16b. The ratio is 1:1 between the bridge and top sites. There are two possible models for the $c(4 \times 2)$ structure, figs. 16c and 16d; the first model assumes 2 bridge sites for each top site and the second model 2 top sites for each bridge site. Figs. 16e and 16f show the models corresponding to those of figs. 16c and 16d with relaxation.

5.4.3. Laser simulation

Fig. 17 shows the laser simulation corresponding to the $p(3\sqrt{2} \times \sqrt{2})R45^\circ$ structure of fig. 16b. The laser diffraction pattern is in good agreement with the LEED diagram.

Fig. 18 shows the laser simulations of the $c(4 \times 2)$ structure corresponding to the models of fig. 16 without relaxation, and with relaxation to take into account the short distance between the pairs of CO on bridge sites. The small differences between all these simulations do not help in deciding between the two models for the $c(4 \times 2)$ structure. Yet it seems that the two non-relaxed models are closer to the LEED patterns.

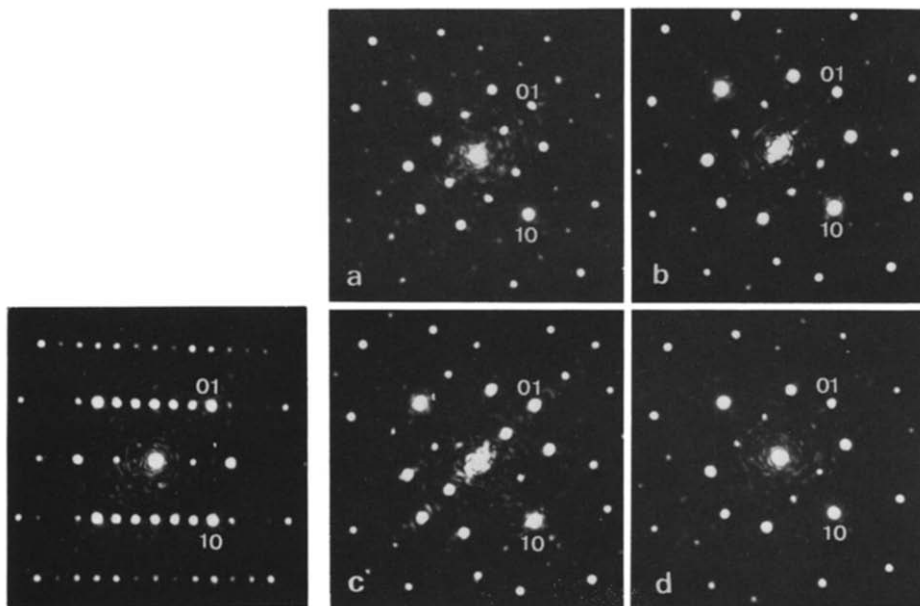


Fig. 17. Laser simulation of the $p(3\sqrt{2} \times \sqrt{2})R45^\circ$ structure of CO on Pt (100).

Fig. 18. Laser simulation of the $c(4 \times 2)$ structure of CO on Pt (100) corresponding to the models of figs. 16c–16f.

5.4.4. Conclusion

For the adsorption of CO on Pt (100), there is no ambiguity in determining the position of the CO molecules for the $c(2 \times 2)$ and $c(3\sqrt{2} \times \sqrt{2})R45^\circ$ structures. For the $c(4 \times 2)$ structure, there are two possible models, and if we assume that the ratio of the number of top site molecules to the bridge sites increases with coverage, then the model of fig. 16d is best suited to describe the surface.

6. General discussion and conclusion

In this paper, we have reexamined the 2D crystallographic arrangements of carbon monoxide adsorbed on (100) surfaces of copper, palladium, nickel and platinum. We have assumed that the CO molecules sit at or very near to specific sites: top or bridge as determined by HREELS or IRS, and that the LEED patterns are formed by coincidence lattices. We have compared the experimentally observed LEED patterns to laser simulations. From our work, it appears that the high symmetry models are more favoured compared to the

compact models. The preferred surface structures are summarized in table 1. This result has a number of consequences:

(i) The "complex" CO structures are formed by ordered antiphase domains of the low coverage high symmetry structure such as $c(2 \times 2)$. This point was first shown by Huber and Oudar [2] in a broad way and applied more specifically to the adsorption of sulfur on the (110) faces of molybdenum [40], the (110) faces of platinum [41] and palladium [42]. This model has also been applied to the adsorption of metals on (100) surfaces of metals [43]. The existence of walls between antiphase domains has been used to explain the non-commensurate structures of rare gases adsorbed on the basal plane of graphite [44–47], and was also proposed for the reconstruction of the (100) surfaces of platinum and gold [48].

(ii) The transition between two consecutive structures as the coverage increases is obtained by unidirectional compression. This behaviour has been predicted theoretically for physisorption on anisotropic substrates [49] and checked experimentally for xenon adsorbed on (110) copper surfaces [50]. For hexagonal symmetry substrates like (0001) graphite surfaces, theory predicts in some cases the existence of parallel walls upon adsorption near the commensurate–incommensurate transition [45,51]. Also uniaxial compression is proposed to explain the LEED patterns of bismuth adsorbed on (100) surfaces of copper [52].

(iii) Some of the CO molecules are separated by distances equal to the diameter of the metal substrate atoms. Most authors have compared CO–CO

Table 1

Preferred models for CO adsorption on fcc (100) surfaces; "strip width" indicates the width of strips with the $1/2$ monolayer coverage structure ($c(2 \times 2)$ or $p(2\sqrt{2} \times \sqrt{2})R45^\circ$), separated by walls with a larger local coverage

Substrate	Unit cell	Top/bridge site occupancies	Strip width in rows	Coverage	Illustrating figure
Cu (100)	$c(2 \times 2)$	1/0	∞	1/2	–
	$c(7\sqrt{2} \times \sqrt{2})R45^\circ$	8/0	4	4/7	3c
	$c(5\sqrt{2} \times \sqrt{2})R45^\circ$	6/0	3	2/3	Similar to 3c
Pd (100)	$p(2\sqrt{2} \times \sqrt{2})R45^\circ$	0/2	∞	1/2	7
	$c(5\sqrt{2} \times \sqrt{2})R45^\circ$	0/6	3	3/5	8b
	$p(3\sqrt{2} \times \sqrt{2})R45^\circ$	0/4	2	2/3	9b
	$c(7\sqrt{2} \times \sqrt{2})R45^\circ$	0/10	2–1	5/7	10b
Ni (100)	$c(2 \times 2)$	1/0	∞	1/2	–
	$c(5\sqrt{2} \times \sqrt{2})R45^\circ$	1/2 or 2/1	–	3/5	13b, c or d
	$p(3\sqrt{2} \times \sqrt{2})R45^\circ$	–	–	–	–
Pt (100)	$c(2 \times 2)$	0/1	∞	1/2	–
	$p(3\sqrt{2} \times \sqrt{2})R45^\circ$	2/2	0	2/3	16b
	$c(4 \times 2)$	3/2	2	5/8	16d

distances to the relatively large Van der Waals diameter of CO, but this is not a correct comparison because the chemisorption involves electron transfer that drastically changes the "diameter" of the molecule. It is preferable to compare the CO-CO distance in chemisorbed CO on metal surfaces to the same distance in metal carbonyls. It has been shown that in some cases, like vanadium carbonyls [53], linearly bonded terminal CO molecules that are parallel to each other are separated by distances of about 2.7 Å, much smaller than the Van der Waals diameter. In biscarbonyl annulene ($C_6H_{10}O_2$), the bridges CO molecules, which are nearly parallel to each other, are at even shorter distances (about 1.5 Å) [54]. It is interesting to note that in the early days of surface science, chemisorbed oxygen and sulfur for example were assumed to have their ionic diameter and that later, LEED intensity calculations have demonstrated that the adsorbed oxygen and sulfur atoms are in fact much smaller. Because of the short distance between the CO molecules, it is tempting to suppose that they shift or tilt on the surface, keeping their bonding bridged or linear. Yet our laser simulations suggest that this is not the case, and that if it happens it is only a secondary effect. As a support for this model for (100) surfaces, a similar analysis of the adsorption of CO on Pt (111) surfaces by HREELS and LEED has been made [55], showing the necessity of CO molecules adsorbed at 2.76 Å distances. A possible consequence of these results is that more compressed structures could be obtained by increasing the adsorption pressure and decreasing the substrate temperature, and ultimately in cases where there is only one type of adsorption site – like linear for Cu (100) and bridged for Pd (100) surfaces – a (1 × 1) structure could be obtained with one CO molecule per metal surface atom.

(iv) Another consequence of our model is that calculations performed to explain the shift of the HREELS or IRS peaks versus coverage using compact models should be reexamined with this new model, since CO molecules are allowed to sit at closer distances and the shifts should be correspondingly larger.

(v) Some accepted coverages may have to be recalibrated.

In conclusion, it appears that the study of the adsorption of CO on metal surfaces is of particular interest for understanding complex surface structures, because of the ability of independent determination of the adsorption sites by HREELS and IRS. The existence of antiphase domains or walls is proved in this case by comparison between LEED and laser simulations. This should encourage more experimental and theoretical work on 2D crystallography. This paper will be followed by a similar paper on the adsorption of CO on (111) fcc surfaces [1], part of which has already been published [56].

References

- [1] J.P. Biberian, and M.A. Van Hove, to be published.
- [2] M. Huber and J. Oudar, *Surface Sci.* 47 (1975) 605.

- [3] J. Pritchard, *J. Vacuum Sci. Technol.* 9 (1972) 895.
- [4] J. Pritchard, T. Catterick and R.K. Gupta, *Surface Sci.* 53 (1975) 1.
- [5] K. Horn and J. Pritchard, *Surface Sci.* 55 (1976) 701.
- [6] B.A. Sexton, *Chem. Phys. Letters* 63 (1979) 451.
- [7] S. Andersson, *Surface Sci.* 89 (1979) 477.
- [8] R.W. Joyner, C.S. McKee and M.W. Roberts, *Surface Sci.* 26 (1971) 303.
- [9] M.A. Chesters and J. Pritchard, *Surface Sci.* 28 (1971) 460.
- [10] J.C. Tracy, *J. Chem. Phys.* 56 (1972) 2748.
- [11] R.C. Brundle, in: *Proc. 7th Intern. Vacuum Congr. and 3rd Intern. Conf. on Solid Surfaces*, Vienna, 1977, p. 1171.
- [12] J. Pritchard, *Surface Sci.* 79 (1979) 231.
- [13] S. Andersson and J.B. Pendry, *Phys. Rev. Letters* 43 (1979) 363.
- [14] J.P. Biberian and M. Huber, *Surface Sci.* 55 (1976) 259.
- [15] A.M. Bradshaw and F.M. Hoffman, *Surface Sci.* 52 (1975) 449.
- [16] F.M. Hoffman and A.M. Bradshaw, in: *Proc. 7th Intern. Vacuum Congr. and 3rd Intern. Conf. on Solid Surfaces*, Vienna, 1977, p. 1167.
- [17] A.M. Bradshaw and F.M. Hoffman, *Surface Sci.* 72 (1978) 513.
- [18] R.L. Park and H.H. Madden, Jr., *Surface Sci.* 11 (1968) 188.
- [19] J.C. Tracy and P.W. Palmberg, *J. Chem. Phys.* 51 (1969) 4852.
- [20] H. Conrad, G. Ertl, J. Koch and E.E. Latta, *Surface Sci.* 43 (1974) 462.
- [21] S.D. Bader, J.M. Blakely, M.B. Brodsky, R.J. Friddle and R.L. Panosh, *Surface Sci.* 74 (1978) 405.
- [22] R.J. Behm, K. Christmann, G. Ertl, M.A. Van Hove, P.A. Thiel and W.H. Weinberg, *Surface Sci.* 88 (1979) L59.
- [23] S. Andersson, *Solid State Commun.* 21 (1977) 75.
- [24] S. Andersson, in: *Proc. 7th Intern. Vacuum Congr. and 3rd Intern. Conf. on Solid Surfaces*, Vienna, 1977, p. 1019.
- [25] J.D. Fedyk, P. Mahaffy and M.J. Dignam, *Surface Sci.* 89 (1979) 404;
J.D. Fedyk and M.J. Dignam, in: *ACS Symp. Ser. No. 137*, Eds. A.T. Bell and M.L. Hair (Am. Chem. Soc., 1980) ch. 5.
- [26] R.L. Park and H.E. Farnsworth, *J. Chem. Phys.* 43 (1965) 2351.
- [27] M. Onchi and H.E. Farnsworth, *Surface Sci.* 11 (1968) 203.
- [28] R.A. Armstrong, in: *Structure and Chemistry of Solid Surfaces*, Ed. G.A. Somorjai (1968) p. 52-1.
- [29] J.C. Tracy, *J. Chem. Phys.* 56 (1972) 2736.
- [30] S. Andersson and J.B. Pendry, *Surface Sci.* 71 (1978) 75.
- [31] M. Passler, A. Ignatiev, F. Jona, D.W. Jepsen and P.M. Marcus, *Phys. Rev. Letters* 43 (1979) 360.
- [32] K. Heinz, E. Lang and K. Müller, *Surface Sci.* 87 (1979) 595.
- [33] S.Y. Tong, A. Maldonado, C.H. Li and M.A. Van Hove, *Surface Sci.* 94 (1980) 73.
- [34] G. Pirug, H. Hopster and H. Ibach, *Ned. Tijdschr. Vacuumtech.* 16 (1978) 2.
- [35] H. Froitzheim, H. Hopster, H. Ibach and S. Lehwald, *Appl. Phys.* 13 (1977) 147.
- [36] C.W. Tucker, Jr., *J. Appl. Phys. Letters* 1 (1962) 34.
- [37] C.W. Tucker, Jr., *Surface Sci.* 2 (1964) 516.
- [38] C.R. Helms, H.P. Bonzel and S. Kelemen, *J. Chem. Phys.* 65 (1976) 1773.
- [39] G. Brodén, G. Pirug and H.P. Bonzel, *Surface Sci.* 72 (1978) 45.
- [40] L. Peralta, Y. Berthier and J. Oudar, *Surface Sci.* 55 (1976) 199.
- [41] Y. Berthier, J. Oudar and M. Huber, *Surface Sci.* 65 (1977) 361.
- [42] L. Peralta, Y. Berthier and M. Huber, *Surface Sci.* 104 (1981) 435.
- [43] J.P. Biberian and M. Huber, *Surface Sci.* 55 (1976) 259.
- [44] P.S. Schabes-Retchkiman and J.A. Venables, *Surface Sci.* 105 (1981) 536.
- [45] H. Shiba, *J. Phys. Soc. Japan* 48 (1980) 211.

- [46] J. Villain, *Phys. Rev. Letters* 41 (1978) 36.
- [47] J. Villain, *Surface Sci.* 97 (1980) 219.
- [48] M.A. Van Hove, R.J. Koestner, P.C. Stair, J.P. Biberian, L.L. Kesmodel, I. Bartos and G.A. Somorjai, *Surface Sci.* 103 (1981) 218.
- [49] V.L. Pokrovsky and A.L. Talapov, *Phys. Rev. Letters* 42 (1979) 65.
- [50] M. Jaubert, A. Glachant, M. Bienfait and G. Boato, *Phys. Rev. Letters* 46 (1981) 1679.
- [51] J. Villain, in: *Ordering in Strongly Fluctuating Condensed Matter Systems*, Ed. T. Riste (Plenum, New York, 1980) p. 221.
- [52] J.P. Biberian, to be published.
- [53] H. Vahrenkamp, *Chem. Ber.* 111 (1978) 3472.
- [54] R. Destro and M. Simonetta, *Acta Cryst.* B33 (1977) 3219.
- [55] N.R. Avery, *J. Chem. Phys.* 74 (1981) 4202.
- [56] J.P. Biberian and M.A. Van Hove, in: *Proc. Conf. on Vibrations at Surfaces*, Namur, 1980, p. 91.